

MINERALOGICAL, GEOCHEMICAL, MICROMORPHOLOGICAL AND SPECTRAL ANALYSES OF QUARTZ SANDSTONES IN NORTHWEST CHAD BASIN, NIGERIA

Öykü ATAYTÜR*, Geological Engineering Department, Faculty of Engineering, Muğla Sıtkı Koçman University, Turkey, ataytur6@gmail.com

([ID](https://orcid.org/0000-0002-2088-7695) <https://orcid.org/0000-0002-2088-7695>)

Ceren KÜÇÜKUYSAL Geological Engineering Department, Faculty of Engineering, Muğla Sıtkı Koçman University, Turkey, cerenkucukuysal@mu.edu.tr

([ID](https://orcid.org/0000-0002-4108-3522) <https://orcid.org/0000-0002-4108-3522>)

Kemal ZORLU, Department of Architecture and City Planning, Kahta Vocational School, Adıyaman University, Turkey, kemalzorlu.geol@gmail.com

([ID](https://orcid.org/0000-0003-2111-4659) <https://orcid.org/0000-0003-2111-4659>)

Aliyu Bashir ALBİŞİR, Geological Engineering Department, Faculty of Engineering, Muğla Sıtkı Koçman University, Turkey, aliyubashir84@gmail.com

([ID](https://orcid.org/0000-0003-1586-8905) <https://orcid.org/0000-0003-1586-8905>)

Murat GÜL, Geological Engineering Department, Faculty of Engineering, Muğla Sıtkı Koçman University, Turkey, muratgul.geol@gmail.com

([ID](https://orcid.org/0000-0003-1555-6426) <https://orcid.org/0000-0003-1555-6426>)

Received: 25.02.2019, Accepted: 09.06.2019

*Corresponding author

Research Article

DOI: 10.22531/muglajsci.531940

Abstract

Here, we present quartz sandstone samples observed from widely distributed, white-coloured, uncemented units in and around Matsena village located in northwest of Chad Basin, NE Nigeria. The mineralogical, geochemical compositions and micromorphological characteristics of the quartz sandstones were determined by X-ray diffraction (XRD), X-ray fluorescence (XRF), stereo microscope and scanning electron microscopy (SEM), respectively. The spectral distribution of these lithological units was determined by using Landsat 8 OLI and image enhancement techniques. XRD and XRF analyses reveal that the quartz sandstone samples can be characterized as mature-super mature by their high SiO₂ contents. General appearances of the quartz grains under SEM show rounded to sub-rounded and to a lesser extent sub-angular habits with dish-shaped cavities, V-shaped depressions, mature conchoidal fractures and linear grooves, all of which suggest the mechanical impact on quartz grains from aeolian, fluvial-marine and colluvial environments.

Keywords: Quartz sandstone, Mineralogy, Landsat, Chad Basin, Nigeria

KUZEYBATI ÇAD HAVZASI, NİJERYA KUVAR S KUMTAŞLARININ MİNERALOLOJİK, JEOKİMYASAL, MİKROMORFOLOJİK VE SPEKTRAL ANALİZLERİ

Özet

Burada, KD Nijerya Çad Havzasının kuzeybatısında yer alan Matsena yerleşimi civarından kuvars kumtaşı örneklerini sunuyoruz. Bu kuvars kumtaşlarının mineralojik, jeokimyasal bileşimi ve mikromorfolojik özellikleri sırasıyla XRD, XRF, stereo mikroskop ve SEM analizleri ile belirlenmiştir. Bu litolojik birimlerin alansal dağılımı Landsat 8 OLI ve görüntü iyileştirme teknikleri ile belirlenmiştir. XRD ve XRF analizleri, kuvars kumtaşı örneklerini, yüksek SiO₂ içeriğinden dolayı olgun- ileri olgun olarak karakterize edilebileceğini göstermiştir. Kuvars tanelerinin SEM ile genel görünüşleri yuvarlaktan yarı yuvarlak ve daha az oranda yarı köşeli morfolojide; çanak şekilli boşluklu, v şeklinde çukurlu, gelişmiş konkoidal çatlaklı ve lineer çizgili morfolojisini gösterir; bunlar da kuvars taneleri üzerinde mekanik etkinin eolien, flüvyal-denizel ve kolüvyal ortamlardan geliştiğini önermektedir.

Anahtar Kelimeler: Kuvars Kumtaşı, Mineraloji, Landsat, Çad Havzası, Nijerya

Cite

Ataytür, Ö., Küçükuysal, C., Zorlu, K., Albishir, A. B., Gül, M. (2019). "Mineralogical, geochemical, micromorphological and spectral analyses of quartz sandstones in northwest chad basin, nigeria ", Mugla Journal of Science and Technology, 5(1), 127-136.

1. Introduction

Chad Basin is the largest intracratonic basin of the Africa, (Fig. 1A,1B) [1-5]. The basin has been subject of

many studies [1-4][6,7]. Among them, some studies were especially focused on the oil and hydrocarbon reservoirs, petroleum geochemistry and organic matter

[4,5][8-15]. The south eastern part of the Chad basin is also called as Bornu Basin [1-5]. The study area is located in NE of Nigeria in Chad Basin (Fig.1A) where the granitic rocks have local exposures, however sedimentary units are widely distributed (Fig. 1B). Especially white-coloured quartz-rich sandstone and red coloured clayey units are recognized in the study

area. However, their compositional variations in the study area have not been studied widely. Therefore, the research problem for this study is to determine the compositional variation of the quartz sandstones and to correlate with the spectral distributions in the study area.

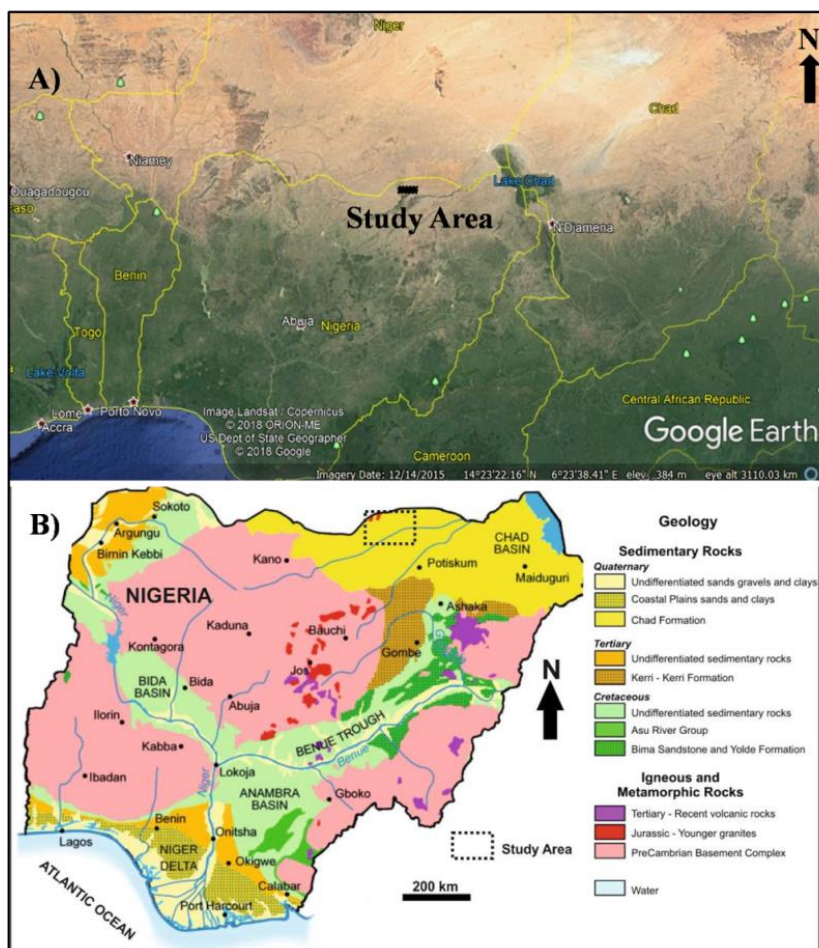


Figure 1. A) Location map of the study area [16], B) General geological map of the study area (from [3] which modified the map from [2]).

2. Geological Setting

The geological map of the region including the study area is taken from [3] which modified the map from [2] whom prepared the map based on data from [17] and [18].

The study area contains Jurassic-Younger Granites and Chad Basin deposits (Fig. 1B) [2, 3]. According to [6], the Younger Granites of Nigeria includes volcanic-granitic ring complexes which contain Jurassic minor peralkaline, metaluminous intrusions and abundant peraluminous biotite-granite. Having a wide distribution in NE of Nigeria, the Chad Basin contains various lithologies. One of them is the Albian-Cenomanian Bima Sandstone Formation which is dominated by continental deposits of poorly sorted and thickly bedded feldspathic sandstones and conglomerates to fluvial and deltaic sediments (Fig. 1B) [1,3]. Furthermore, early Turonian aged continental

basal and marine sediments of limestones, sandstones and shales form up the Gongila Formation in the basin [1,3,4]. Another unit in the basin is the Senonian-Maastrichtian Fika shale Formation that consists of both marine and continental originated gypsiferous shales [1] and limestone [3]. The Maastrichtian Gombe Sandstone Formation is composed of estuarine-deltaic deposits of siltstone-mudstone-ironstone at the bottom, coals and cross bedded sandstone in upper part and overlies the Palaeocene Kerri-Kerri Formation deposits of lacustrine or fluvio-lacustrine claystones, siltstones, ironstones, lignite and conglomerates (Fig. 1B) [3].

Being the youngest deposit in the basin, the Chad Formation (Pliocene-Pleistocene age) is comprised of the continental units of poorly sorted, fine to coarse grained sand, sandy clay and diatomite (Fig. 1B) [1,3,4]. [1] found that uncemented angular and subangular, fine to coarse-grained, yellow, brown, white to grey coloured

quartz grains are dominant in the formation. Additionally, the presence of massive and locally sandy clay deposits in the study area was correlated with the presence of sand bodies which corresponds to the Lower-Middle-Upper Aquifer Zones proposed by [19]. The Upper Aquifer Zone contains recent alluvium and aeolian sands and gravels [3]. Macroscopically the Younger Granite exposures are seen in the study area and shown in Figure 2A. The weathering on the granite bodies produced red clay having 4-5 m thickness in the study area (Fig. 2A). The granite body with visible

crystal sizes of the minerals and overlying weathering products are shown in Figure 2B.

Macroscopic observations on the granite samples show medium-coarse quartz crystals, K-feldspars and biotite crystals with clear cleavage surfaces. Approximately 2-3 m thick white-coloured sandstone units are observed throughout the study area in a close surrounding region of the Matsena village. M1, M2, M3 and M4 samples were obtained from this quartz bearing deposits (Fig. 2C).



Figure 2.A) Younger Granite exposures with red clay in the study area, B) the granite body and overlying weathering products, C) sample location of M1.

3. Materials and Methods

3.1. Field Study

The field study was performed in and around Matsena village, which is located to the south of the boundary between southeast Niger and northeast Nigeria. The geological map of the area (Fig. 1B) showed that this region is covered by the Chad Formation. The Younger Granite exposures in the study area (Fig. 2B), their weathering zones as red clays on top of the granites (Fig. 2A) and widely distributed quartz sandstones (Fig. 2C) were all observed during the field study. The samples of M1, M2, M3 and M4 were taken from white coloured uncemented sandstone units to the southwest of the granite body.

3.2. Data and Image Processing Methods

Landsat 8, launched on 11 February 2013, is the latest in a continuous series of land remote sensing satellites that began in 1972. The cloud-free Landsat 8 OLI satellites scenes path 187 / row 51 (acquired time: 24 April 2018) and path 188 / row 51 (acquired time: 01 May 2018) downloaded from USGS Earth Resources

Observation and Science web site were used for determining the spectral distribution of quartz sandstones, granites and red clay in the study area. Digital image processing was carried out by using Envi software. Image enhancement methods as contrast enhancement [20], panchromatic sharpening, band rationing and colour composite techniques [21] were applied to geometrically and radiometrically corrected, mosaicked and extracted images. Band rationing is a technique where the digital number value of one band is divided by the digital number value of another band [22]. It was applied successfully in several studies dealing with lithology discrimination and hydrothermal alteration mapping [23-26]. Following band ratios are usually used for extracting geological and lithological features [27-31]. Clay Minerals Ratio, 6/7 (SWIR1/SWIR2) Landsat 8 OLI band ratio highlights hydrothermally altered and hydroxyl bearing rocks containing kaolinite and alunite [28]. Ferrous Minerals Ratio, 6/5 (SWIR/NIR) Landsat 8 OLI band ratio highlights iron-bearing minerals [27, 28]. Iron Oxide Ratio, 4/2 (RED/BLUE) Landsat 8 OLI band ratio

highlights hydrothermally altered rocks that have been subjected to oxidation of iron-bearing sulphides [27, 28].

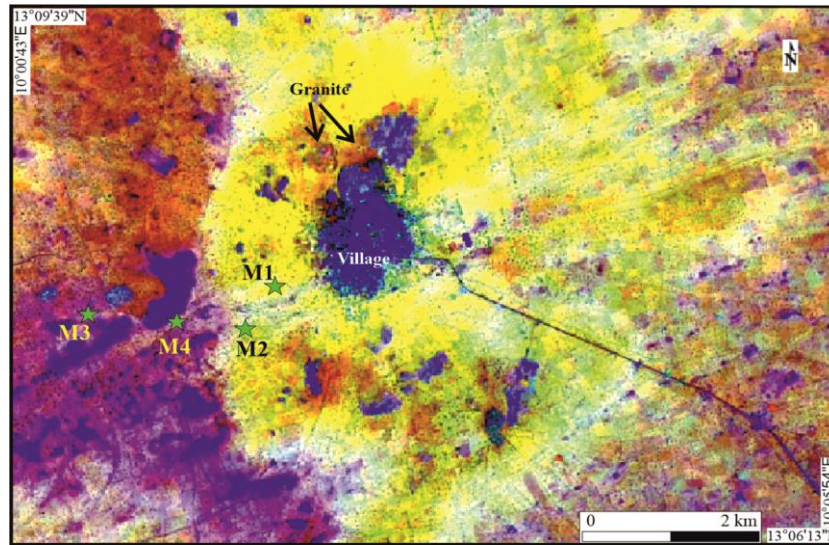


Figure 3. Younger Granite ring structure and sample points in Landsat 8 OLI RGB 742 colour composite.

3.3. Laboratory Analysis

Samples were analyzed mineralogically by Panalytical Expert Pro diffractometer equipped with a Cu tube at 40kV voltage and 30mA current with a scanning rate of 2°/min in Mineralogy-Petrography Laboratory at General Directorate of Mineral Research and Exploration. Combined procedures of [32-36] were followed during preparation of the samples for X-ray diffraction. The separated <2µm size fraction was mounted as aggregates on glass slides for M1 sample [37]. Four X-ray patterns were recorded as air-dried (AD), ethylene glycol solvated for 24h (EG) and heated at 350°C (350°C) and 550°C (550°C) for 2h. The diffractograms were plotted between 4° -70° 2θ for the whole rock samples and between 2°-42° 2θ for the fine fraction (<2µm) of M1. Whole rock chemical analysis of major elements was performed by using Rigaku ZSX Primus II XTF equipment at Advanced Technology Education Research and Application Centre at Mersin University. Scanning Electron Microscope Analysis was carried out at Research and Application Centre for Research Laboratories at Muğla Sıtkı Koçman University. The specimens were sputter coated with gold (Emitech K550X Sputter Coating Systems). Samples were examined under a scanning electron microscope (SEM) (Jeol JSM-7600F, Japan) at an accelerating voltage of 15 kV. Elemental characterizations of the samples were done using the SEM equipped with Energy Dispersive X-ray Spectrometry (EDS-Oxford Instruments). Microscope images of the samples were

observed under MOTIC model stereo microscope to better characterize the morphology and homogeneity of mineral grains.

4. Results

4.1. Image Interpretation

Eight different RGB colour composite images prepared from single bands and rationed bands for image interpretation and to discriminate geological units for this study. These RGB colour composites are 4/2_6/7_5, 4/3_6/2_7/3, 6/7_5/4_7/5, 432, 652, 674, 742 and 764. The geological units studied are visible best in RGB 742 colour composite (Fig. 3). The ring-shaped structure of the Jurassic-Younger Granite exposure in the study area can easily be lineated to the north of the Matsena village (Fig. 3) and viewed in pink colour; additionally the red clay can be observed in brown colour in RGB 652 colour composite (Fig. 3). Very wide distribution of the yellow colour is suggested to match with the distribution of quartz sandstones in the study area (Fig. 3).

4.2. XRD Analysis

The bulk diffractogram of the samples reveal monomineralic phase for M1 and M2 in that only the prominent peaks of quartz were observed as of 3.34 Å, 4.25 Å, 2.45 Å, 2.28 Å and 1.81 Å (Fig.4). In addition to quartz mineral present in M3 and M4 samples, clay mineral peak at 4.49Å for both; calcite at 3.01 Å and dolomite at 2.90 Å for M3 and calcite at 3.02 Å and feldspar at 3.24 Å for M4 were identified (Fig.4).

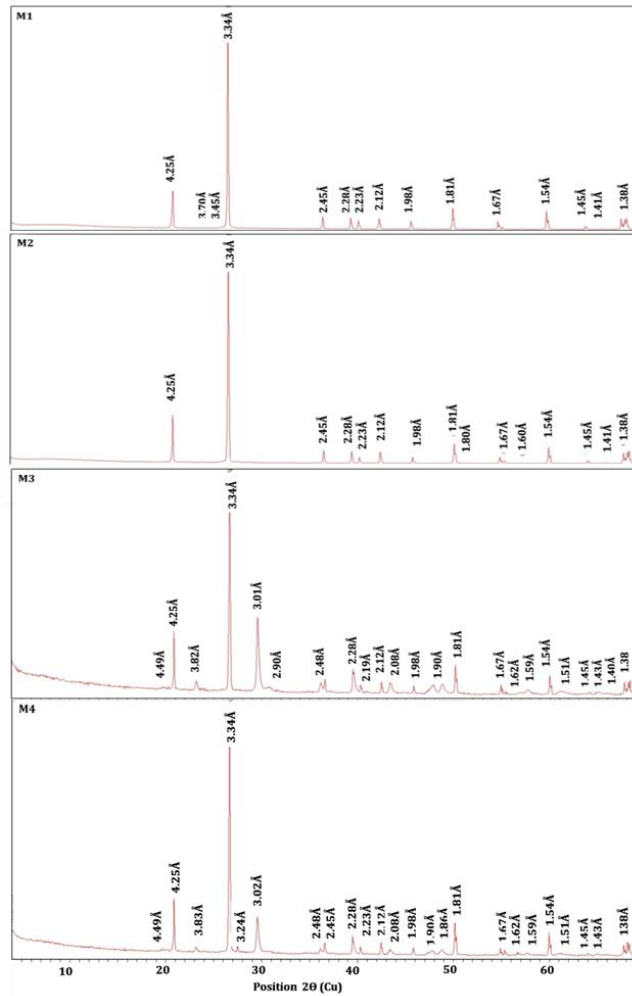


Figure 4. X-ray diffractograms of whole rock samples of M1,M2,M3 and M4.

In the x-ray diffractograms of the sample M1's fine fraction, the same peaks support the presence of quartz as single crystalline phase in very close surrounding to the granite body (Fig.5).

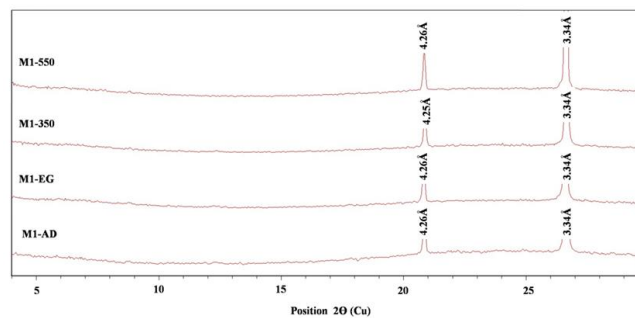


Figure 5. X-ray diffractograms of the clay fraction of sample M1 (AD: air dried; EG: ethylene glycol solvated; 350°C: heated to 350°C; 550°C: heated to 550°

4.3. XRF Analysis

Major oxide compositions of the samples reveal that SiO₂ amount is very high for all samples (Table 1). Also, the samples are depleted in terms of alkali elements. Fe₂O₃ composition was recorded as nearly 1% for each sample (Table 1). The presence of calcite in M3 and M4 is supported by CaO amount (4.35 – 2.65%). These data are compatible with the mineralogical findings in that

the samples are mostly dominated with quartz grains some of which are coated with iron crust.

Table 1. Major oxide compositions of the studied samples; M1,M2,M3,M4.

Weight (%)	Na ₂ O	MgO	Al ₂ O ₃	SiO ₂	P ₂ O ₅	K ₂ O	CaO	TiO ₂	Fe ₂ O ₃	LOI
M1	0.01	0.53	0.78	96.57	0.01	0.05	0.05	0.14	1.00	0.65
M2	<0.01	<0.01	1.27	97.15	0.02	0.07	0.06	0.19	0.74	0.36
M3	<0.01	0.75	1.16	89.58	<0.01	0.12	4.35	0.14	0.92	2.73
M4	0.14	0.55	1.23	92.38	<0.01	0.13	2.65	0.15	0.89	1.72

4.4. SEM-EDS Observations

General view of rounded, sub-rounded and rare sub-angular quartz grains [38] is shown in Fig.6A,E,G and I. In Fig.6B,H and I, dish-shaped depressions are shown; V-shaped cavities, on the other hand, are observed in Fig.6B,D and F [39-42]. Subangular-subrounded quartz

grains with mature conchoidal fracture [39,40,42,43] surfaces in Fig.6C and rare linear grooves in Fig.6C,F [43,44] are also observed. Holes on a single well-rounded quartz grain are shown in Fig.6D [39-42].

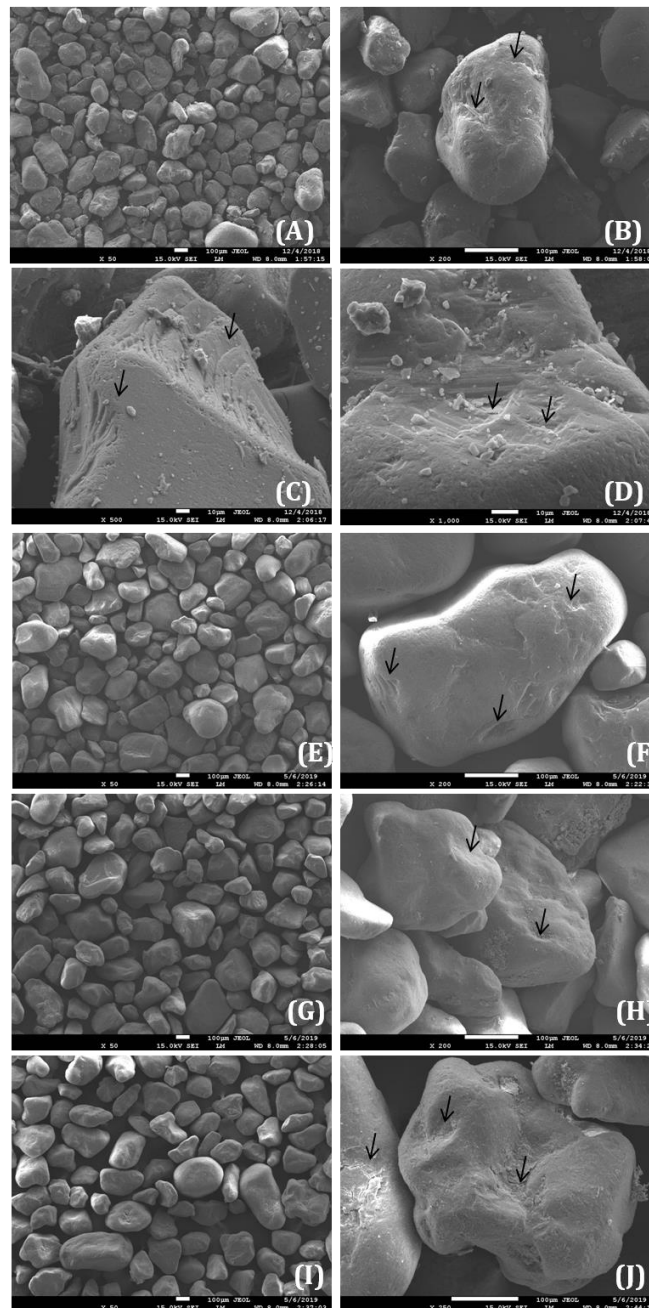


Figure 6. A, E, G, I) General view of rounded-subrounded and subangular quartz grains, B) Well-rounded quartz grain from M1 showing dish-shaped depressions and V-shaped cavities, C) M1; Subangular - subrounded quartz grain with

mature conchoidal fracture surfaces and linear grooves, D) M1; Well-rounded quartz grain with V-shaped cavities and holes, E) General view of M2 sample having subrounded to rounded quartz grains, F) General view of M2 sample having rounded quartz grain with linear grooves and V-shaped cavities, G) General view of M3, subangular subrounded quartz grains, H) M3; Dish shaped cavities on some grains and rest is dull quartz grains, I) General view of M4 rounded to subrounded quartz grains J) M4; Dish shaped cavities and surficial deformation patterns of sample

4.5. Microscopic Determinations

Stereomicroscope photomicrographs of the samples are shown in Fig.7. Rounded and sub-rounded quartz grains with rare Fe-O coatings [45] and grayish-black colored sub-angular minerals were all observed under microscope (Fig.7). Iron bearing coating is suggested to be due to non-crystalline form of iron.

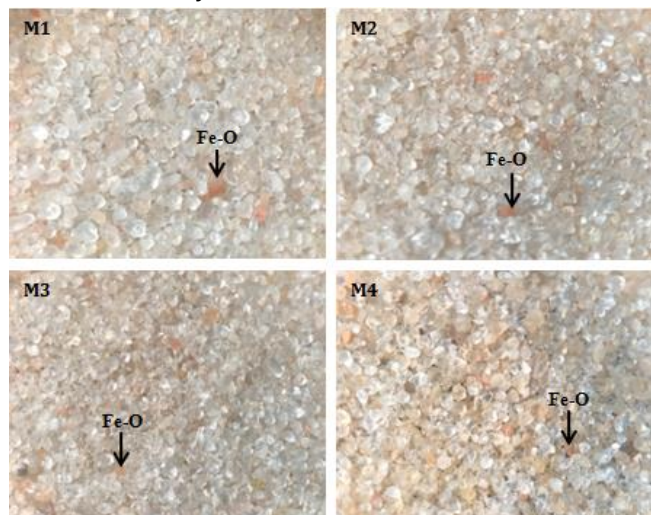


Figure 7. The stereomicroscope photomicrographs of samples M1,M2,M3,M4 (x20 magnification; Fe-O: iron-oxide coating on quartz grains).

5. Discussion

SEM investigations reveal the quartz morphologies and also the presence of possibly a diatom fragment (?) attached onto a single quartz grain in M1 (Fig.8A), EDS of which also confirms high Si content (Fig. 8B). This information correlates with the knowledge given by [46] in that the sand fraction of the Early Pliocene middle aquifer sediments was reported to include moderate to coarse grained quartz, Fe-oxides, interbedded clays and diatoms. Mineral assemblages of the samples show two distinct groups in that M1 and M2 has only quartz in their compositions, however, M3 and M4 samples have dominantly quartz together with minor calcite, dolomite and feldspar; all of which are supported with the geochemical findings. Very low amount of Fe is sufficient to colour some quartz grains, as well. The Fe content of the samples is suggested to be originated from the middle aquifer sediments of Chad Formation [46].

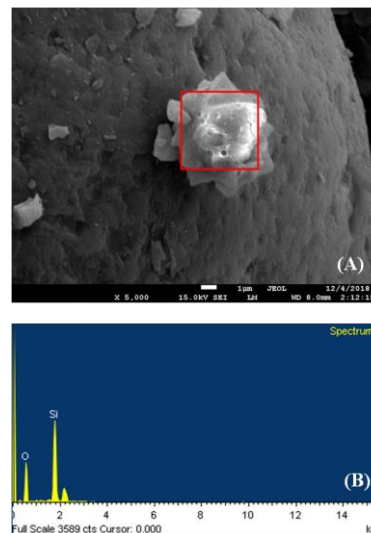


Figure 8.A) The diatom fragment (?) attached on a rounded edge of a quartz grain of M1, B) EDS spectrum on the diatom fragment (?).

Micromorphological analyses on the quartz grains of the samples show various observations. [1] stated that the uncemented quartz grains with angular and sub-angular habits belong to Chad Formation. However, SEM observations clearly present that the samples are not only composed of sub-angular quartz grains; they also include rounded to sub-rounded quartz grains with dish-shaped depressions together with V-shaped cavities [39-42], mature conchoidal fracture surfaces [42] and linear grooves [43, 44]. These morphological observations imply the mechanical impacts occurred in aeolian [3], fluvial (Bima and Kerri Kerri Formations; [1, 3]), marine (Gongila Formation; [1,3,4]) and colluvial (Upper Aquifer Zone sediments; [3]), environments [39-42].

The spectral analysis on the study area and its close surrounding shows the restricted distribution of the red clay on and around the granite bodies (Fig. 3). On the other hand, the quartz sandstone units are determined to have very wide distribution in the study area as well as in southern part of Chad Basin (NE Nigeria). Field observations suggest the contribution of quartz grains from Jurassic Younger Granite exposures; however, the micromorphological observations on the roundness and surface features of the quartz grains allow suggesting much greater possibility of longer transportation distance from different possible source rocks (Bima, Kerri Kerri and Gongila Formations). [47] defines silica sand deposits with more than 95% quartz as mature or super mature. Based on this definition, the studied samples can be classified as mature -super mature high purity deposit.

As a common knowledge, quartz sand is widely used in various industrial applications; however, their suitability depends on many different parameters [47], which is not the scope of this paper. Being a mature and super mature quartz sandstones with almost negligible compositions of Al, Mg, Ca and K (elements affect the melting properties) and not greater than 1% of Fe₂O₃ are all favorable requirements to suggest the quartz sandstones in the study area for economical applications like glass, water filtration, aerated concrete, foundry material and ceramics, etc. [47].

6. Conclusion

According to the mineralogical, geochemical and micromorphological findings, the quartz sandstones from Chad Basin is suggested to be the member of Chad Formation. They are classified as mature - super mature and high purity deposits. Due to its very wide distribution in the region and the chemical purity, this mature and super mature quartz sandstones are suggested to be evaluated as possible economical raw materials for industrial applications. As a conclusion, this study recommends further investigations to better understand the suitability of the quartz sandstones for different industrial applications.

7. Acknowledgment

We thank Assist. Prof. Dr. Mehmet Ali KURT (Mersin University-Turkey) for the assistance with XRF analyses of the samples. The reviewers of this contribution are highly acknowledged due to their invaluable comments which significantly improved the quality of the manuscript. This research did not receive any specific grant from funding agencies.

8. References

- [1] Okosun, E.A., "Review of the Geology of Bornu Basin", *Journal of Mining and Geology*, 31(2), 113-122, 1995.
- [2] MacDonald, A.M., Cobbing, J. and Davies, J., "Developing groundwater for rural water supply in Nigeria: a report of the May 2005 training course and summary of groundwater issues in the eight focus states", *British Geological Survey*, 32pp, 2005. (CR/05/219N) (Unpublished).
- [3] Adelana, S.M.A., Olasehinde, P.I., Bale, R.B., Vrbka, P., Edet, A.E. and Goni, I.B., "An overview of the geology and hydrogeology of Nigeria", In: Adelana, S.M.A., Mac Donald, A. (Eds.), *Applied Groundwater Studies in Africa. IAH Selected Papers on Hydrogeology*, 13,171-197, 2008.
- [4] Mohammed, Y.B. and Tela, B., "Assessment of Tertiary Sediments of Bornu Basin for Possible Hydrocarbon Reservoir", *Research Journal in Engineering and Applied Sciences*, 1(4), 251-257, 2012.
- [5] Olabode, S.O., Adekoya, J.A. and Ola, P.S., "Distribution of sedimentary formations in the Bornu Basin, Nigeria", *Petroleum Exploration and Development*, 42(5), 674-682, 2015.
- [6] Van Breemen, O., Hutchinson, J. and Bowden, P., "Age and Origin of the Nigerian Mesozoic Granites: ARb-Sr Isotopic Study", *Contributions to Mineralogy and Petrology*, 50 (3), 157-172, 1975.
- [7] Adegoke, A.K., Sarki Yandoka, B.M., Abdullah, W.H. and Akaegbobi, I.M., "Molecular geochemical evaluation of Late Cretaceous sediments from Chad (Bornu) Basin, NE Nigeria: implications for paleo depositional conditions, source input and thermal maturation", *Arabian Journal of Geosciences*, 8(3), 1591-1609, 2014.
- [8] Ekweozor, C.M., Okosun, J.I., Ekong, D.E.U. and Maxwell, J.R., "Preliminary organic geochemical studies of samples from Niger Delta, Nigeria", Part 1: Analysis of crude oils for triterpanes, *Chemical Geology*, 27, 11-28, 1979.
- [9] Doust, H. and Omatsola, E., "Niger Delta", In: Edwards J.D., Santogrossi P.A., (eds) *Divergent/passive Margin Basins, AAPG Memoir 48, American Association of Petroleum Geologists, Tulsa*, 239-248, 1990.
- [10] Mohamed, A.Y., Pearson, M.J., Ashcroft, W.A., Illiffe, J.E. and Whiteman, A.J., "Modeling petroleum generation in the Southern Muglad rift basin, Sudan", *AAPG Bulletin*, 83(12), 1943-1964, 1999.
- [11] Peters, K.E. and Fowler, M.G., "Applications of petroleum geochemistry to exploration and reservoir management", *Organic Geochemistry*, 33, 5-36, 2002.
- [12] Seewald, J.S., "Organic-inorganic interactions in petroleum-producing sedimentary basins", *Nature*, 426,327-333, 2003.
- [13] Obaje, N.G., Wehner, H., Scheeder, G., Abubakar, M.B. and Jauro, A., "Hydrocarbon prospectivity of Nigeria's inland basins: from the viewpoint of organic geochemistry and organic petrology", *AAPG Bulletin*, 88(3), 325-353, 2004.
- [14] Peters, K.E., Walters, C.C. and Moldowan J.M., "The biomarker guide: biomarkers and isotopes in petroleum exploration and earth history", second eds, vol 2. Cambridge University Press, Cambridge, 2005.
- [15] Akinlua, A., Ajayi, T.R., Adeleke, B.B., "Organic and inorganic geochemistry of northwestern Niger Delta oils", *Geochemical Journal*, 41,271-281, 2007.

- [16] Google Earth Pro, NE Nigeria. 14° 23'22.16"N 6°23'38.41"E. Eye alt 3110.03 km. Image Landsat/Copernicus 2018 (December 14, 2015).
- [17] UNESCO, Geological map of Africa (1: 5000, 000). UNESCO, Paris, 1987.
- [18] Geological Survey of Nigeria, "Geological Map of Nigeria 1:2.000000", Geological Survey of Nigeria, Kaduna, 1984.
- [19] Barber, W. and Jones, D.G., "The geology and hydrology of Maiduguri, Bornu Province", *Record of the Geological Survey Nigeria*, 1960.
- [20] Rao, T.C.M., Ven kataratnam, L. and Rao, K.R., "Contrast enhancement of landsat data on multispectral data analysis system", *Journal of the Indian Society of Photo-Interpretation and Remote Sensing*, 8(2), 27-32, 1980.
- [21] Kalelioğlu, Ö., Zorlu, K., Kurt, M.A. Gül, M. and Güler, C. "Delineating compositionally different dykes in the Ulukışla basin (Central Anatolia, Turkey) using computer - enhanced multi - spectral remote sensing data", *International Journal of Remote Sensing*, 30(11), 2997-3011, 2009.
- [22] Inzana, J., Kusky, T., Higgs, G. and Tucker, R., "Supervised classifications of Landsat TM band ratio images and Landsat TM band ratio image with radar for geological interpretations of central Madagascar", *Journal of African Earth Sciences*, 37, 59-7, 2003.
- [23] Hunt, G.R., Salisbury, J.W. and Lenhoff, C.J., "Visible and near-infrared spectra of minerals and rocks", VI. Additional silicates, *Modern Geology*, 4, 85-106, 1973.
- [24] Hunt, G.R. and Ashley, R.P., "Spectra of altered rocks in the visible and near infrared", *Economic Geology*, 74, 1613-1629, 1979.
- [25] Hunt, G.R., "Electromagnetic radiation: the communication link in remote sensing", In Siegal, B.S., Gillespie, A.R., (Eds), *Remote Sensing in Geology*, 5-45 (New York: Wiley), 1980.
- [26] Hunt, G.R. and Hall, R.B., "Identification of kaolins and associated minerals in altered volcanic rocks by infrared spectroscopy", *Clays and Clay Minerals*, 29, 76-78, 1981.
- [27] Segal, D.B., "Theoretical Basis for Differentiation of Ferric-Iron Bearing Minerals, Using Landsat MSS Data", In Proceedings of the International Symposium on Remote Sensing of Environment, 2nd Thematic Conference, *Remote Sensing for Exploration Geology*, 6-10 December, Fort Worth, TX, vol. II (Ann Arbor, MI: Publications Environmental Research Institute of Michigan), 949-951, 1982.
- [28] Drury, S., "Image Interpretation in Geology", London: Allen and Unwin, 243 pp, 1987.
- [29] Sabins, F.F., "Remote sensing for mineral exploration", *Ore Geology Reviews*, 14(3-4), 157-183, 1999.
- [30] Han, T. and Nelson, J., "Mapping hydrothermally altered rocks with Landsat 8 imagery : A case study in the KSM and Snow field zones , northwestern British Columbia", In: Geological Fieldwork 2014, British Columbia Ministry of Energy and Mines, *British Columbia Geological Survey Paper*, 2015-1, pp.103-112, 2015.
- [31] Mwaniki, M.W., Moeller, M.S. and Schellmann, G., "A comparison of Landsat 8 (OLI) and Landsat 7 (ETM+) in mapping geology and visualising lineaments: A case study of central region Kenya", *International Archives of the Photogrammetry, Remote Sensing and Spatial Information Sciences*, XL-7/W3, 897-903, 2015.
- [32] Brindley, G.W., "Quantitative X-Ray Analyses of Clays", In: Brindley, G. W., Brown, G., (Eds), *Crystal Structures of Clay Minerals and Their X-Ray Identification*, Mineralogical Society Monograph, 5, 411-438, 1980.
- [33] Jackson, M.L., "Soil Chemical Analysis-Advanced Course, 2nd Edition", Published by the Author, Madison, Wisconsin, 895, 1979.
- [34] Moore, D.M. and Reynolds, J.R., "X-Ray Diffraction and the Identification and Analysis of Clay Minerals", Oxford University Press, 332, 1989.
- [35] Thorez, J., "Practical Identification of Clay Minerals: a handbook for teachers and students in clay mineralogy", Lelotte, Dison, Belgium. 90, 1976.
- [36] Tucker, M., "Techniques in Sedimentology", Blackwell Scientific Publications, 394, 1988.
- [37] Moore, D.M. and Reynolds, R.C., "X-ray diffraction and identification and analysis of clay minerals", Oxford University Press, 135, 819-842, 1997.
- [38] Welton, J.E., "SEM Petrology Atlas, Methods in Exploration", Series No. 4, The American Association of Petroleum Geologists, 237, 2003.
- [39] Tadeusz, S., Rybka, R.S. and Woronko, B., "Upper Pleistocene and Holocene deposits at Starunia paleontological site and vicinity (Carpathian region, Ukraine)", *Annales Societatis Geologorum Poloniae*, 79(3), 255-278, 2009.

- [40] Al-Dousari, A.M. and Al-Hazza, A., "Physical properties of Aeolian sediments within major dune corridor in Kuwait", *Arabian Journal of Geosciences*, 6(2), 519–527, 2013.
- [41] Calvo, F.R., Sánchez, J., Acosta, A., Wolf, D. and Faust, D., "Granulometrical, mineralogical and geochemical characterization of loess deposits in the Tajo Basin", *Quaternary International*, 407, 14–28, 2016.
- [42] Újvári, G., Kok, J. F., Varga, G. and Kovács, J., "The physics of wind-blown loess: Implications for grain size proxy interpretations in Quaternary paleoclimate studies", *Earth-Science Reviews*, 154, 247–278, 2016.
- [43] Pavelić, D., Kovačić, M., Banak, A., Jiménez-Moreno, G., Marković, F., Pikelj, K., Vranjković, A., Premužak, L., Tibljaš, D. and Belak, M., "Early Miocene European loess: A new record of aridity in southern Europe", *Geological Society of America Bulletin*, 128(1-2), 110-121, 2015.
- [44] Kleesment, A., "Roundness and surface features of quartz grains in Middle Devonian deposits of the East Baltic and their palaeo geographical implications", *Estonian Journal of Earth Sciences*, 58(1), 71-84, 2009.
- [45] Ali, A.M., Padmanabhan, E. and Baioumy, H., "Incorporation of silica into the goethite structure: a microscopic and spectroscopic study", *Acta Geochimica*, 37(6), 911-921, 2018.
- [46] Obaje N.G., "The Bornu Basin (Nigerian Sector of the Chad Basin), In: Geology and Mineral Resources of Nigeria", Lecture Notes in Earth Sciences, vol 120. Springer, Berlin, Heidelberg, 2009.
- [47] Platias, S., Vatalis, K.I. and Charalampides, G., "Suitability of Quartz Sands for Different Industrial Applications", *Procedia Economics and Finance*, 14, 491-498, 2014.